A&A 371, 932–942 (2001)
DOI: 10.1051/0004-6361:20010386

Astronomy & Astrophysics

Hα emission line spectroscopy in NGC 330⋆

On the hybrid model for global oscillations in Be star circumstellar disks

W. Hummel[1,6], W. Gässler[1,7], B. Muschielok[1], H. Schink[2], H. Nicklas[2], G. Conti[3], E. Mattaini[3], S. Keller[4], K.-H. Mantel[1], I. Appenzeller[5], G. Rupprecht[6], W. Seifert[5], O. Stahl[5], and K. Tarantik[1,8]

[1] Institut für Astronomie und Astrophysik und Universitäts-Sternwarte München, Scheinerstr. 1, 81679 München, Germany
[2] Universitäts-Sternwarte Göttingen, Geismarlandstr. 11, 37083 Göttingen, Germany
[3] CNR – Istituto Fisica Cosmica, Via Bassini 15, 20133 Milano, Italy
[4] Mount Stromlo Observatory, Private Bag, Weston Creek, Weston, ACT 2611, Australia
[5] Landessternwarte Heidelberg, Königstuhl 12, 69117 Heidelberg, Germany
[6] European Southern Observatory, Karl-Schwarzschildstr. 2, 85748 Garching, Germany
[7] National Astronomical Observatory of Japan, Saburo Telescope, 650 North A'ohoku Place, Hilo, Hawaii, HI 96720 USA
[8] Max-Planck-Institut für extraterrestrische Physik, Postfach 1312, 85741 Garching, Germany

Received 4 October 2000 / Accepted 1 March 2001

Abstract. We perform an observational test on global oscillations in Be star circumstellar disks in the metal deficient environment of the SMC. According to the hybrid model of disk oscillations early-type Be stars require an optically thin line force to establish a density wave. The low metallicity in the SMC should therefore diminish or prevent the formation of disk oscillations in early-type Be stars. We present short wavelength range spectra around Hα of 48 Be stars in the young open cluster NGC 330 in the SMC. We find that the fraction of early-type Be stars in NGC 330 which host a global disk oscillation does not differ from the known fraction of Galactic field Be stars. This observational result is in contradiction to the theoretical prediction. We discuss several interpretations and propose a further observational test.

Key words. line: formation, profiles – stars: circumstellar matter, emission-line, Be

1. Introduction

About 1/6−1/3 of all Galactic B-type stars with luminosity class III–V once showed Hα in emission and have therefore been classified as Be stars (Zorec & Briot 1997; Jaschek & Jaschek 1981). The hydrogen, He I and singly ionized metallic emission lines originate in a circumstellar gaseous quasi-Keplerian disk. The formation of the rotating disk is associated with episodic mass-loss events (e.g. Rivinius et al. 1998), however the Be star mass-loss mechanism is not yet known. Low resolution (Dachs et al. 1986) as well as high resolution spectroscopy of individual emission lines (Hanuschik et al. 1996) has provided valuable information on the structure, kinematics and evolution of Be star circumstellar disks in the Galaxy (e.g. Telting 2000 for a review).

A considerable fraction of all Galactic field Be stars exhibit a long term variable so-called V/R asymmetry (V/R means the ratio of the violet to the red continuum-subtracted peak intensity in a double peak line profile) in their emission lines with a mean cycle of 6.8 years (Copeland & Heard 1963) while the remaining fraction show symmetric emission lines. Hanuschik (1988) extended the terminology of long V/R-variables and called them Class 2 line profiles to account for asymmetric and long-term variable single-peak profiles which share the same physical phenomenon seen at low inclination (see Hanuschik et al. 1995), while symmetric line profiles without V/R variability are called Class 1. The cyclic behavior of Class 2 emission lines was for a long time a matter of debate (for a discussion see Ballereau & Chauville 1989)

Send offprint requests to: W. Hummel,
e-mail: whummel@eso.org

⋆ Based on observations collected with VLT-Kueyen-FORS2-MXU during the commissioning 1 of FORS2 and the mechanical commissioning of the MXU, operated on Cerro Paranal (Chile) by the European Southern Observatory and the VLT instrument consortium (FORS2).

but is now interpreted as due to one-armed global oscillations in a nearly Keplerian circumstellar disk (Okazaki 1991, 1997; Papaloizou et al. 1992; Savonije & Heemskerk 1993). The model predictions were confirmed by observations (Hanuschik et al. 1995; Telting et al. 1994; Hummel & Hanuschik 1997; Mennickent et al. 1997).

These waves are confined to the inner region of the circumstellar disk and the confinement radius is predicted to amount to ≃10–15 stellar radii (Savonije 1999; Okazaki 1997, 2000) in agreement with results based on line profile modeling (Hummel 2000a).

In the hybrid model for global disk oscillations (hereafter GDOs) for viscous decretion disks (Okazaki 1997, hereafter O97) two different mechanisms are proposed to confine a GDO. For the late-type Be stars a quadrupole of the potential induced by the rotationally flattened star provides a deviation from the purely Keplerian flow to establish the necessary confinement constraint as proposed by Papaloizou et al. (1992). Since early-type Be stars (MK B0-B4) do not rotate as close to the critical break-up velocity as late type Be stars (MK = B5-B9) (Fukuda 1982) the quadrupole of the potential as due to rotational flattening is no longer efficient for MK=B0-B4. For early-type Be stars the optically thin line force of the stellar radiation is proposed to perform the wave confinement to establish GDOs (O97).

In this study we present an observational test for the hybrid scenario. The efficiency of the optically thin line force depends on the metallicity of the central star. The terminal velocity in winds of O stars in the SMC is usually about 1000 $\mathrm{km\,s^{-1}}$ lower with respect to their Galactic counterparts (Garmany et al. 1985; Haser et al. 1998). Kudritzki et al. (1987) interpreted the lower terminal velocity as due to a lower line force and a four times lower wind momentum assuming $Z_{\rm SMC} = 0.1\ Z_\odot$, ($Z_\odot = 0.02$, Cox 2000). We selected the young open cluster NGC 330 in the SMC, since it is one of the best studied SMC clusters and shows a large number fraction of Be/(B+Be) stars (Feast 1972; Grebel et al. 1992; Keller et al. 2000). Furthermore the metallicity of this cluster is supposed to be even lower than in the field around NGC 330, hence enhancing the metallicity effect to be studied (Grebel & Richtler 1992). Hill (1999) found $Z = 0.004$ for NGC 330 and $Z = 0.006$ for the field around NGC 330, meaning $Z_{\rm NGC\ 330} = 0.2$–$0.3\ Z_\odot$.

The relation between the optically thin line force F and the metallicity Z is not well known. For B supergiants and O-type stars F scales something between linear and square root with the metallicity (Pauldrach & Puls, priv. comm.):

$$F \sim Z^{\frac{1}{2}\cdots 1} \tag{1}$$

meaning that the optically thin line force can be estimated to be $0.2-0.45$ (for the field) and $0.1-0.3$ (for the cluster) of the Galactic value for solar abundance.

As a consequence the confinement constraint for GDOs around early-type Be stars in the SMC is predicted to be considerably reduced with respect to Galactic Be stars. The prediction of the hybrid model would be a larger confinement radius and a larger oscillation period, or even a complete lack of GDOs in early-type Be stars.

The hybrid scenario can therefore easily be tested by a comparison between the number fraction of Be stars with long-term V/R-variability (Class 2 Be stars, N II) to the total number of all Be stars

$$N_{V/R} = \frac{\mathrm{N\,II}}{\mathrm{N\,I+II}} \tag{2}$$

where N I+II is the total number of all Be stars showing either long-term V/R-ratio variations (=Class 2) or not (=Class 1). We thereby assume that $N_{V/R}$ is dependent on the general requirements for GDOs, like the confinement, and on the unknown excitation mechanism, since GDOs are not self-exciting. We furthermore assume the unknown excitation mechanism for GDOs to be equal for all Be stars and that the observed $N_{V/R}$ measures how far the physical requirements for GDOs are met.

2. Observation preparation

2.1. Be star catalogs for NGC 330

For the present study we selected Be stars mainly from two catalogs: Grebel (1995) and Keller et al. (1999). The distance modulus of the SMC is $m - M_V = 18\overset{\rm m}{.}9$ (Grebel 1995) and Keller et al. (2000) used $m - M_V = 18\overset{\rm m}{.}85$. The 116 Be stars detected by Grebel (1995) range from $V = 14\overset{\rm m}{.}4$ to $V = 18\overset{\rm m}{.}9$ which corresponds to spectral types B0 to B6 using the calibration of Zorec & Briot (1991). Be stars detected by Keller at al. (1999) range from $V = 14\overset{\rm m}{.}4$ to $V = 17\overset{\rm m}{.}5$ corresponding to spectral types B0 to B3. This means that all targets of Keller et al. (1999) and those targets of Grebel (1995) with $V^{\rm m} < 18\overset{\rm m}{.}25$ (G1-G103) belong to the spectral classes B0-B4 under consideration.

2.2. Astrometry

Our preparation image used for the observations with FORS2 was obtained a year earlier with FORS1 (Hummel et al. 1999) with a field of view of 6.8×6.8 arc min. Four targets of the astrometric catalog of Tucholke et al. (1996) were in the field of the preparation image and were used to calibrate the astrometric scale. The catalogues of Grebel (1995) and of Keller et al. (1999) were cross-correlated using the finding charts and a new astrometric target list was created. The image distortion of FORS1 was taken into account when deriving astrometric positions for the Be stars in the field of NGC 330. Our astrometry shows a mean offset of $\Delta\alpha = 0\overset{\prime\prime}{.}8$ and $\Delta\delta = 0\overset{\prime\prime}{.}9$ with respect to the catalog of Keller et al. (1999).

2.3. Selection effects, and completeness

Only one setup was prepared, meaning a subset of targets was selected from the catalogs on the basis of an

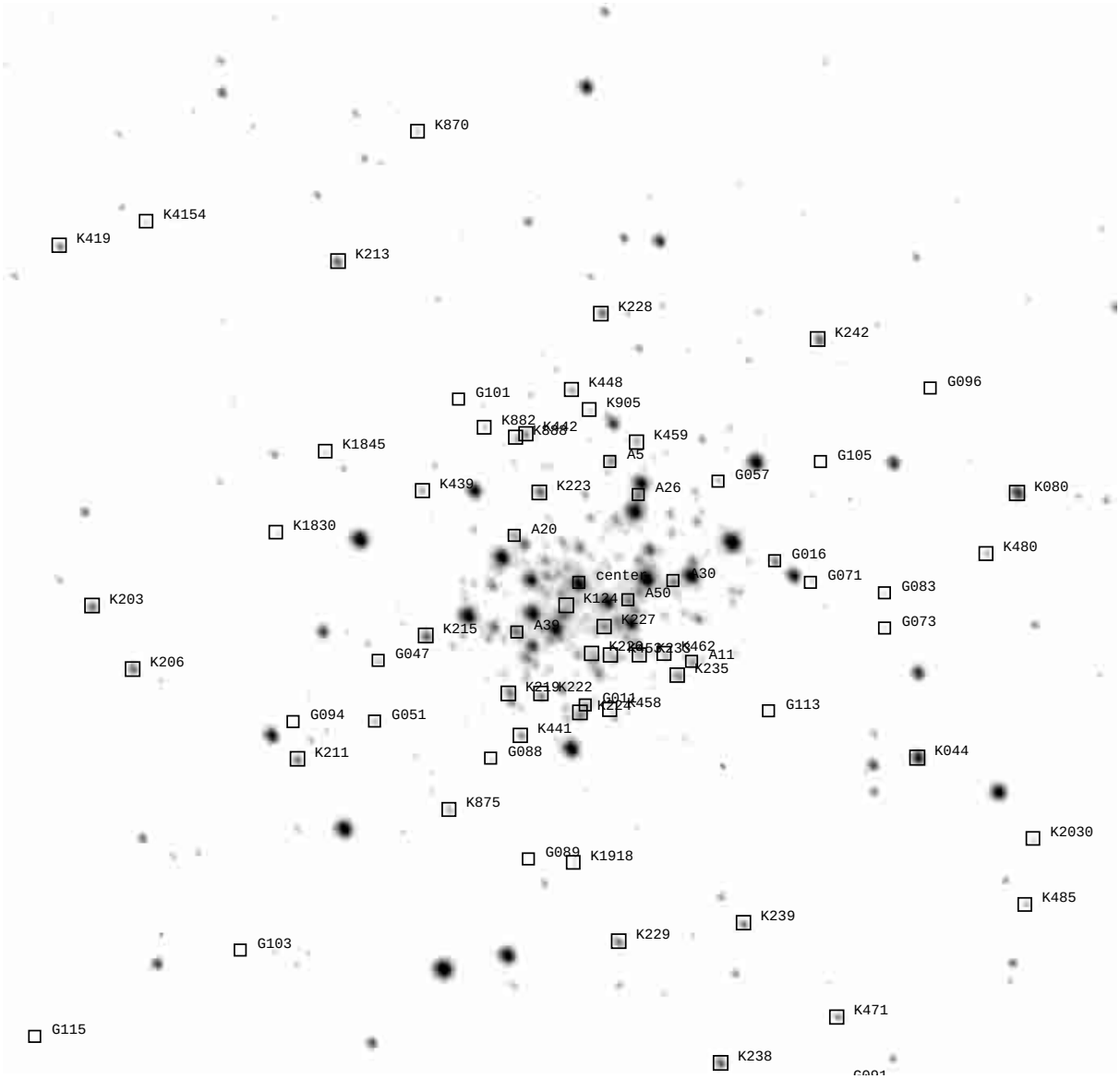

Fig. 1. Central part ($2.3' \times 2.3'$) of the preparation image ($6.8' \times 6.8'$) obtained with FORS1 at Antu (former UT1) and position of photometrically identified Be stars. North is top and East is left. Prefixes: A, B from Roberts (1974), K from Keller et al. (1999) and G from Grebel (1995)

optimum geometrical solution for the slit positions in the field of view. Since we limited the fully available spectral range of the 600R+24 grism by the Hα interference filter H_Alpha+59 which provides a bandwidth of $\Delta\lambda = 60$ Å, we could place several slits side by side without overlapping the spectra on the CCD.

The completeness of this study can be estimated to be around 40% for the early-type Be stars B0-B4 in NGC 330.

2.4. Mask production

Slit positions for the mask were defined using FIMS (Hummel 2000b) and the mask was produced together with technical masks for the commissioning some weeks before the observations with the VIRMOS Mask Manufacturing Unit (Conti et al. 1999). We used a common slit width of 0.26 mm corresponding to 0.5 arcsec.

3. Observations

The spectroscopic observations were collected as two 900 s exposures with FORS2 in MXU mode at VLT Kueyen (former UT2) on Paranal as part of the first commissioning period of the instrument. The instrument is described by Böhnhardt (2000), and Seifert et al. (2000), while the mask exchange unit (MXU) of FORS2 is described by Schink et al. (2000). The nominal pointing was RA = 00:56:19.043, DEC = −72:27:59.81 for the instrument setup. Up to 7 reference stars were used to align the telescope pointing to the correct position. Additionally

Table 1. Log of observations. From left to right: Julian date, date and UT at start of observation, FORS2 instrument modus, grism, interference filter and central wavelength, exposure time, approximative seeing and air mass

JD	date	UT	mode	grism	filter	λ_c nm	time sec	seeing arcsec	X
2451494.15	12/11/99	03:38	MXU	600R+24	H_Alpha+59	656	900	0.8	1.5
2451494.16	12/11/99	03:54	MXU	600R+24	H_Alpha+59	656	900	0.8	1.5

a reference slit was specified to correct the image flexure of the instrument. The wavelength range coverage is 6 533 Å $< \lambda <$ 6 593 Å. Most of the slits were longer than 8 arcsec, providing sufficient sky background. Some slits were occupied with two or more targets. Four slits were inclined with respect to the dispersion direction to optimize the sky background region and the spectra required an additional row-by-row alignment handling using the wavelength calibration. The log of observations is given in Table 1. Thanks to the negligible image flexure of FORS2 calibration frames could be collected a day earlier during day-time with the telescope in zenith position.

4. Data reduction

The data reduction was performed using ESO MIDAS SW (Banse et al. 1983). All frames were filtered to eliminate the cosmic ray events and were corrected for bias and flat field. Each spectrum was individually extracted from the science frame, and the same region of the CCD was extracted from the wavelength calibration frame. The background was defined on both sides of the science target if possible and an average background spectrum was subtracted. This simple procedure was justified, since the sky and interstellar background was homogeneous along the slits for all targets, except for the slits with G96 and K255 which showed a rather inhomogeneous Hα background with respect to other background lines. The nebulous objects K799 and K4153 also showed inhomogeneous Hα and [NII] line strengths, most probably due to a spatially resolved circumstellar shell. There were only three Neon lines in the short wavelength range of the calibration frame: λ 6506.5278, 6532.8799, and 6598.9531. We also collected calibration frames with the two Hα interference filters H_Alpha/2500+60 and H_Alpha/4500+61 (red shifted with respect to λ_0 = 6563 Å by 2500 and 4500 km s^{-1} respectively) to collect more calibration lines. It turned out that the three Neon lines in the H_Alpha+59 filter band were sufficient to define a linear wavelength dispersion relation. Spectra were transformed into a velocity scale. A heliocentric correction of $V_{\rm earth} = -12.6$ km s^{-1} was applied. The short wavelength range spectra of G12, G38, G64, G84 G96 and W2:79 suffer from a bad CCD column, accidently located close to Hα.

5. Results

5.1. General

Most of the photometrically identified emission line objects can be confirmed to show Hα in emission. K799 shows [NII] in emission and can therefore no longer be classified as a Be star.

W4:31 and W2:79 show traces of a rotationally broadened stellar absorption profile without any signature of emission, although these stars were classified as emission line objects by photometry. Taking the bright Be star A22 (= G5 = K223 = W1:15) as a reference with a color index of F555W-F656N = $0\overset{\rm m}{.}236$ (Keller et al. 2000) the colors of $0\overset{\rm m}{.}36$ and $-0\overset{\rm m}{.}25$ for W4:31 and W2:79 respectively, would indicate strong emission at least for W4:31.

G108 and G113 also show traces of a rotationally broadened stellar absorption profile without any signature of emission. The *R*-Hα color index of A22 is given as $0\overset{\rm m}{.}46$ (Grebel 1995). The colors of $0\overset{\rm m}{.}22$ and $0\overset{\rm m}{.}10$ for G108 and G113 would indicate a 80% lower Hα emission strength with respect to A22. Note that G108 did not show emission also a year earlier (Hummel et al. 1999, their Fig. 1e) when observed with FORS1.

The status of K255 and G96 remains unclear due to the large fraction of the interstellar contribution to Hα. After subtraction of a homogeneous background for G96 one third of the raw Hα emission was found to be of stellar origin for the FORS1 observations (Fig. 3). The FORS2 observations showed a rather inhomogeneous background. Moreover the box shape of the residual Hα profile indicates an interstellar origin. Spectra of G28, G64 and G111 suffer from low S/N.

Measured *FWHM* of Hα emission range from 590 km s^{-1} (G84) to 150 km s^{-1} (K1830). Note that the *FWHM* of the instrumental profile of 2.7 Å corresponds to 120 km s^{-1}. Hα emission strengths and line shapes (Fig. 2, Table 2) are very similar to those of Galactic Be stars, in particular when compared with surveys of similar spectroscopic resolution (Dachs et al. 1986). A simple preliminary classification with respect to line profile asymmetry is given in Table 2.

5.2. Line profile variability

In Fig. 3 we show the new observations presented in this study together with line profiles obtained a year earlier with FORS1. The spectral resolution of the present Hα line profiles is a factor 2 higher than of those profiles

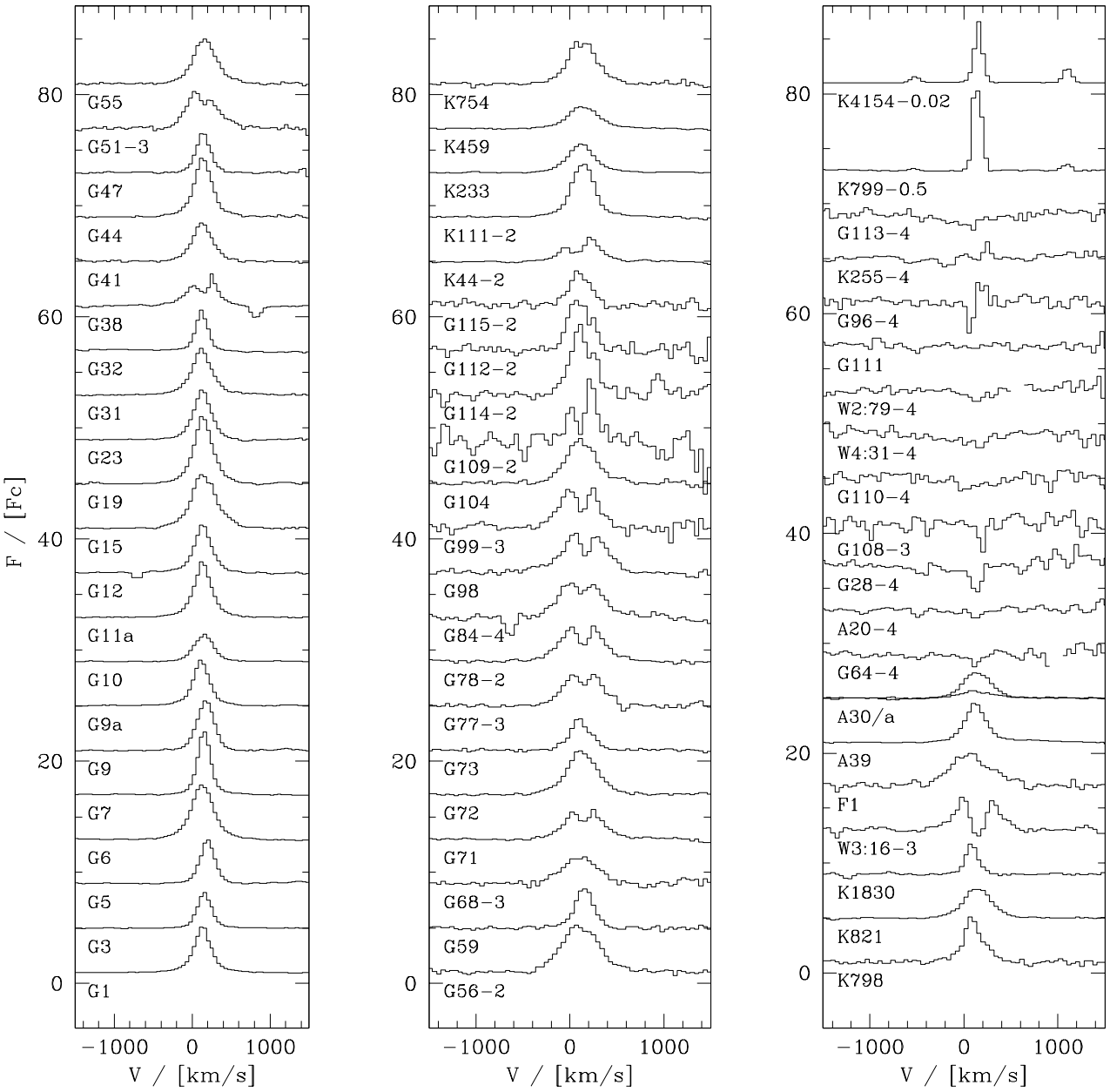

Fig. 2. Spectra of 62 targets in the region of Hα normalized to the local stellar continuum F_c. Spectra are offset in ordinate by multiples of 4.0 F_c. The abscissa gives geocentric velocities. Prefixes: G after (Grebel 1995), K after (Keller at al. 1999), W after (Keller et al. 2000), A, B after (Roberts 1974), and F after (Hummel et al. 1999). The number after the "-" in the name indicates an intensity scaling factor used in the plot for better visibility. Some spectra (G12, G38, G64, G28, G84, W2:79) still contain a bad column residual, which could not be corrected by the flat fielding due to non-linearities

obtained a year earlier. No significant variability is detected for G1, G32, G41, G55, G77, and G78. F1, G109, and G115 show signatures of a change in the profile shape. Decreasing emission equivalent width is found in G9, G59, and G68. The only candidate for a long-term V/R-ratio variability in Fig. 3 is G109, however a time scale of one year is not long enough to detect V/R variability in Be stars.

5.3. Emission line statistics

33 of the 48 line profiles in emission (G96, K799, K4151 and A30a excluded) showed single peaks. Among the 15 double peak profiles six are clearly asymmetric (d/aa) and two further ones show asymmetry with a V/R-ratio close to 1 (d/a). This means that $N_{V/R}$ amounts to 40%−53% for the sufficiently resolved double peak profiles. We found six marginally asymmetric (s/a) and two strongly asymmetric (s/aa) single peak profiles meaning 6% to 24% (2−8 of 33) of the single peak profiles.

We assumed that the number of long-term V/R-variables which are accidently caught during a symmetric phase does bias the number statistics for single peak and double profiles in the same way. Furthermore we assumed that asymmetric profiles with very low $v \sin i$ cannot be

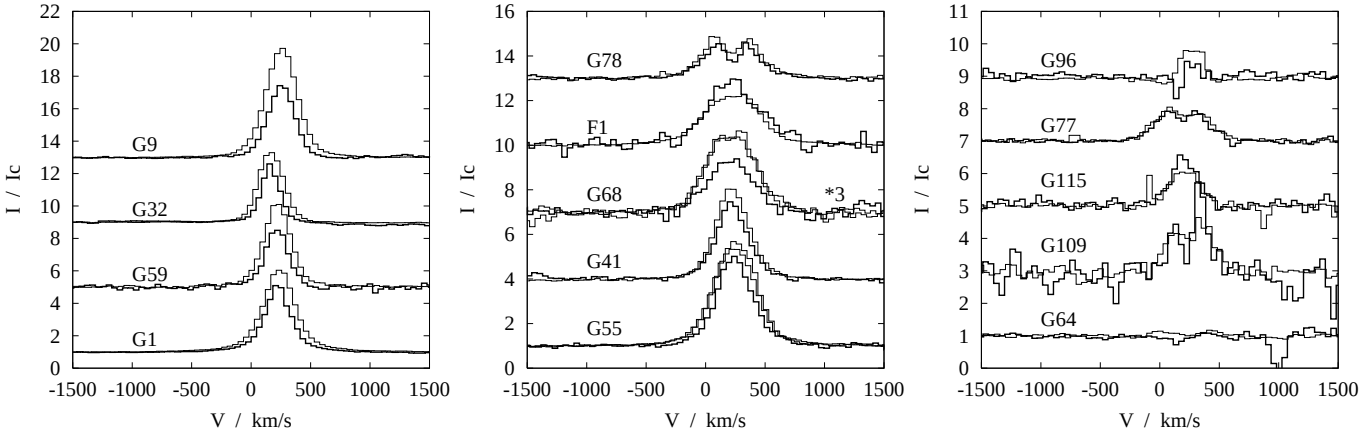

Fig. 3. Variablity of Hα emission line profiles of Be stars in the field of NGC 330. Bold: profiles of the present study collected in Nov./1999 with a spectral resolution of $\Delta V = 120$ km s^{-1} with FORS2 at UT2 in MXU mode. Thin: Profiles of our first study (Hummel et al. 1999) collected in Oct./1998 with a spectral resolution of $\Delta V = 225$ km s^{-1} with FORS1 at UT1 in MOS mode. Profiles of the present study were shifted in V to match the observed velocity of the profiles obtained earlier. Target numbers after Grebel (1995)

detected, also not in high-resolution spectroscopy, since the kinematical broadening is less than the non-kinematical broadening. This selection effect, being independent of the spectral resolution, biases all statistics in the same manner and cancels out when compared to the statistics of other studies.

A further selection effect is that the empirical minimum Hα equivalent width for GDO is $W_\alpha = -10$ Å (Hanuschik et al. 1995). Circumstellar disks with lower W_α are probably physically not able to establish a GDO at all. This empirical result most probably reflects a lower limit for the viscosity which provides the required interaction between different particle trajectories to establish a GDO. We assume that the fraction of Be stars with densities below the critical density for GDOs is independent of inclination and spectral type.

The lower number of $N_{V/R}$ for the single peak profiles with respect to the double peak profiles is therefore due to the finite resolution alone[1]. Taking the statistics for the double peak profiles as representative, we find:

$$N_{V/R}^{\mathrm{NGC\ 330}} = 0.47 \pm 0.13 \tag{3}$$

where 0.47 is the mean value of both statistics (counting the d/a profiles as Class 2 profiles or not) and ±0.13 is given by the standard error for the binomial probability distribution:

$$\sigma = \sqrt{n_{\mathrm{I}} N_{V/R} \mathrm{N\,I+II}}. \tag{4}$$

Thereby we assume the sample amounts to N I + II, and the parent population, the number of all Be stars in NGC 330, is more than twice as large as the sample. n_{I} is the probability to find a Be star of Class 1 in the sample, hence

$$n_{\mathrm{I}} = \frac{\mathrm{N\,I}}{\mathrm{N\,I+II}} \tag{5}$$

and

$$n_{\mathrm{I}} + n_{V/R} = 1. \tag{6}$$

6. Discussion

Some of the Galactic Be stars change from Class 2 to Class 1 and vice-versa (e.g. β^1 Mon, 28 Tau and 66 Oph), meaning disk oscillations can damp out or can start in an initially unperturbed circumstellar disk. It is therefore reasonable to define the number of Be stars with Class 2 lines at a certain epoch.

In Cols. 3–5 of Table 3 we collected $N_{V/R}$ of different emission line surveys of the Galaxy. Only Copeland & Heard (1963) and Hanuschik et al. (1988) give numbers for $N_{V/R}$. The values of the other references and N I + II and N I were derived by simply counting the number of asymmetric line profiles. Known binary stars such as ϕ Per, ζ Tau and HR 2142 were excluded. From Table 3 (Cols. 3–5) we find

$$N_{V/R}^{\mathrm{Gal}} = 0.33 \pm 0.06 \quad (\mathrm{O9{-}B9}) \tag{7}$$

as the relative number of Class 2 disk for Galactic field Be stars. By contrast the number of Be stars that ever showed V/R-ratio variability is much larger (O97). The value of Copeland & Heard (1963) deviates from the mean of the other references, since their observation epoch of 24 years is more than twice as large as the largest epoch of the other studies. The second reason for their larger value of $N_{V/R}$ is that Hβ is used for that study for which V/R variations are easier to detect. Therefore that study is not taken into account for Eq. (7).

The number statistics $N_{V/R}$ for Galactic Be stars as given in Col. 5 of Table 3 is biased in two ways with respect

[1] G1 was spectroscopically not resolved (Mazzali et al. 1996) with EFOSC at $\Delta\lambda = 3.7$ Å (=167 km s^{-1}) but with CASPEC at $\Delta\lambda = 0.33$ Å (=15 km s^{-1}). G1 is an example for a Class 2 profile hidden in the group of single peak profiles. G1 in taken to be a symmetric single peak profile in this study.

Table 2. Hα emission line parameters. From left to right: MXU slit number, target names (prefixes: A, B from Roberts 1974, K from Keller et al. 1999, G from Grebel 1995, F from Hummel et al. 1999, W from Keller et al. 2000 and LIN from Lindsay 1961), emission equivalent width of Hα in Å, peak radial velocity (p) if single peak (comment = s) or velocity of the violet peak (V) the central depression (c) and red peak (R) in case of double peak (comment = d), $FWHM$ in km s^{-1}, intensity of the of profiles in units of the local stellar continuum, comment: s) symmetric single-peak, d) symmetric double-peak, d/aa) asymmetric double peak, s/aa) asymmetric single peak, s/a) marginally asymmetric single peak, d/a) marginally asymmetric double peak, neb) [N II] line emission, abs) no emission, stellar absorption profile, −) low S/N , no classification possibles, [a)]) only V and R given, [b)]) blend with neighbor star, [c)]) 2 stellar components

slit	name	W_α Å	V_p or $V_V/V_\mathrm{c}/V_R$ km s^{-1}	$FWHM$ km s^{-1}	I_p or $I_V/I_\mathrm{c}/I_R$ I_c	comment
72	A20	0	−	−	−	abs
38	F1	32	−70/20/110	500	3.6/3.6/3.9	d/a
20	G1, K80, B21	27	110	260	5.2	s
44	G3, K242, B17	18	150	220	4.2	s
70	G5, K223, A22	24	210:	230	4.9	s
25	G6, K238, B35	43	130	340	5.8	s
15	G7, K213, B12	29	150	200	6.6	s
56	G8, A39	20	130	260	4.1	s [b)]
08	G9, K258	28	160	270	5.4	s
66	G9a, K203, B6	26	120	250	5.0	s
62	G10, K228, B14	18	160	300	3.4	s
49	G11a, K206, B5	33	130	290	5.9	s
22	G12, K229, B36	28	140	320	5.2	s [b)]
21	G15, K480, A24	43	110	360	5.8	s/a
52	G19, K211, B41	52	140	300	7.0	s [b)]
71	G20, A30[c)]	20	140	350	3.3	s
	(G20):, A30a	6	80	400	1.4	s
23	G23, K239, B34	28	120	280	5.4	s
55	G28, K441	−	−	−	−	−
24	G31, K471	29	120	280	5.2	s
13	G32, K419, B9	18	120	190	4.6	s
69	G38, K439	24	30/160/260	380	2.8/2.1/3.9	d/aa
06	G41, K874	26	110	320	4.4	s [b)]
50	G44, K875	37	140	290	6.3	s
54	G47	19	140	280	4.4	s
53	G51	9	30/160/230	470	2.0/1.7/1.8	d/aa
07	G55, K857	34	160	360	5.0	s
36	G56	20	70	460	3.1	s/aa
09	G59, K991	21	160	230	4.5	s
12	G64, K870	0	−	−	−	abs
65	G68	8	110	440	1.8	s/a
68	G71	24	30/160/250	500	3.4/2.6/3.7	d
51	G72, K1845	37	120	380	4.9	s/a
19	G73	17	110	270	3.8	s/a [b)]
47	G77, K1918	10	30/160/250	500	1.9/1.6/1.9	d
46	G78, K2030	17	20/150/250	510	2.6/1.7/2.6	d
34	G84	8	20/120/250	590	1.8/1.5/1.7	d
43	G96	−	−	−	−	f
59	G98	40	70/260/300	500	4.5/2.5/4.2	d/a
37	G99	11	-30/140/250	570	2.2/1.6/2.2	d
35	G104	35	120	360	5.0	s/aa
26	G108	0	−	−	−	abs

a) only V and R given.
b) blend with neighbor star.
c) 2 stellar components.

Table 2. continued. Hα emission line parameters

slit	name	W_α Å	V_p or $V_V/V_\mathrm{c}/V_R$ km s^{-1}	$FWHM$ km s^{-1}	I_p or $I_V/I_\mathrm{c}/I_R$ I_c	comment
57	G109	10	10/120/200	280	2.4/1.2/3.7:	d/aa
42	G110	0	–	–	–	abs
58	G111	–	–	–	–	–
17	G112	14	70/250[a)]	370	3.2/2.5[a)]	d/aa
45	G113	0	–	–	–	abs
05	G114	20	100/190/240	310	4.1/2.7/2.9	d/aa [b)]
29	G115	10	70	320	2.6	s/a
18	K44, B31	8	−70/240[a)]	460	1.6/2.1[a)]	d/aa
30	K111	17	140	270	3.4	s
67	K233	26	120	330	3.6	s [b)]
64	K255, B18	–	–	–	–	f
63	K459	18	140	370	2.9	s
31	K754	32	70/120/170	360	4.8/4.3/4.6	d [b)]
28	K798	23	95	250	5.1	s/a
61	K799	–	–	–	–	neb
60	K821	22	140	340	3.6	s
48	K1830	10	80	150	3.7	s
14	K4154, (LIN 305)	–	–	–	–	neb
11	W2:79	−1	160:	–	0.5:	abs
10	W3:16	8	−20/160/320	500	2.0/0.8/1.9	d
73	W4:31	0	–	–	–	abs

Table 3. Number statistics of $N_{V/R}$ for Galactic samples

		MK = [O9-B9]			MK = [O9-B4]			MK = [O9-B4] $\Delta V_\mathrm{p}^\alpha < 120$ km s^{-1}		
Ref.	epoch	N I+II	N II	$N_{V/R}$	N I+II	N II	$N_{V/R}$	N I+II	N II	$N_{V/R}$
Copeland & Heard (1963)	1938–1962	54	36	0.67	—	—	—	—	—	—
Andrillat & Fehrenbach (1982)	1980–1981	61	24	0.40	33	4	0.12	13	6	0.46
Andrillat (1983)	1981	52	13	0.25	29	5	0.17	9	2	0.22
Hanuschik et al. (1988)	1982, 1985	36	5	0.14	30	12	0.40	10	3	0.30
Doazan[a)] et al. (1991)	1978–1988	96[a)]	33[a)]	0.34[a)]	47	11	0.23	23	5	0.21
Slettebak et al. (1992)	1989	40	15	0.38	25	17	0.68	9	2	0.22
Hanuschik[b)] et al. (1996)	1982–1993	69	25	0.36	46	14	0.30	20	5	0.25

a) Hβ is used in case Hα is not available.
b) Including the study of Slettebak et al. (1992).

to $N_{V/R}$ for NGC 330. First $N_{V/R}^\mathrm{Gal}$ contains also late-type Be stars. To account for this difference we derived $N_{V/R}^\mathrm{Gal}$ again, but now only for the early type stars (see Cols. 6–8 of Table 3). We find

$$N_{V/R}^\mathrm{Gal} = 0.26 \pm 0.1 \qquad (\mathrm{O9{-}B4}) \tag{8}$$

for the Galactic early-type Be stars alone.

The second difference between the Galactic and the NGC 330 number statistics is that $N_{V/R}^{\mathrm{NGC\ 330}}$ in Eq. (3) is for the resolved double-peak profiles alone, which selects mostly the large $v \sin i$ Be stars in NGC 330 (more precisely: the large ΔV_p Be stars in NGC 330, where ΔV_p is the Hα peak separation). Assuming that the observed $v \sin i$ distribution of Be stars is a product of the geometric effect of random axis orientation and of the distribution of relative equatorial rotation velocity

$$w = \frac{v^\mathrm{equ}}{v^\mathrm{crit}}, \tag{9}$$

among individual stars, we suspect Eq. (3) favors Be stars with either a large absolute rotation velocity (equivalent to most early-type Be stars) and/or with a large w, where $v^{\rm equ}$ is the equatorial velocity of the star and $v^{\rm crit}$ is the theoretical break-up velocity. The latter group of large w Be stars shows again the largest oblateness, for which GDO can be established also in a metal-deficient environment. A reduced radiation pressure would therefore not diminish the formation of GDOs. On the other hand the peak separation $\Delta V_{\rm p}$, as a measure of the outer disk radius visible in Hα does mean neither a large $v \sin i$ of the underlying star nor a large w.

Nevertheless we tune the Galactic sample of Be stars for the conditions under which $N_{V/R}^{\rm NGC\ 330}$ was derived and calculated $N_{V/R}^{\rm Gal}$ again, but take only Be stars into account for which MK = [O9-B4] and for which the Hα peak separation of the double peak profile $\Delta V_{\rm p} > 120$ km s^{-1}. So far we adapt the instrumental resolution of FORS2 to the Galactic emission line sample. We find (see Cols. 9–11 of Table 3):

$$N_{V/R}^{\rm Gal} = 0.28 \pm 0.12 \quad ({\rm O9{-}B4}; \Delta V_{\rm p} > 120\ {\rm km\,s^{-1}}) \quad (10)$$

for the Galactic early-type Be stars with the same instrumental selection effect as the statistics for NGC 330.

Our detailed number statistics for the Galactic Be stars show that:

- The relative number of Be stars with V/R-variability, $N_{V/R}^{\rm Gal}$, is independent on spectral type. We suggest that any difference between $N_{V/R}^{\rm NGC\ 330}$ and $N_{V/R}^{\rm Gal}$ can therefore not be caused by selection effects of a different spectral type distribution within the sample;
- For Galactic early-type Be stars, $N_{V/R}^{\rm Gal}$ does not differ for our sample of $\Delta V_{\rm p} > 120$ km s^{-1} with respect to the sample which takes Be stars with any value of $\Delta V_{\rm p}$. This result cannot be used to argue in how far the selection effect on large w Be stars does bias the statistics, since for the Galaxy it is assumed that the radiation pressure causes the confinements of GDOs independent if the second mechanism, the oblateness of the star, does work or not. We can only argue that there is no further intrinsic bias on $N_{V/R}^{\rm Gal}$ when considering only $\Delta V_{\rm p}$ Be stars with $\Delta V_{\rm p} > 120$ km s^{-1}.

Comparing Eq. (7) and Eq. (10) we find as the main result of this study that the fractional number of Be star disks with Class 2 emission lines $N_{V/R}$ in NGC 330 is not significantly reduced with respect to the Galaxy. Hence the occurrence of disk oscillations in the metal-deficient environment of the SMC indicates that an optically thin line force seems not to be required to establish GDOs, in contradiction to the hybrid scenario for GDOs.

We see three possible explanations for the discrepancy in the $N_{V/R}$ number statistics.

1. The metallicity of about $Z_{\rm SMC} = 0.2\ Z_{\rm Gal}$ might not be low enough to diminish the line force by the necessary amount to cut off the conditions for disk waves.
   The results of Kudritzki et al. (1987) show that the ratio of weak lines to strong lines (=α wind parameter) is mostly independent on the metallicity for $30\,000 \leq T_{\rm eff} \leq 40\,000$ meaning that the weak line force is locked with the metallicity.
   If the metallicity of the SMC is not sufficiently low to diminish the line force the conditions to establish disk oscillations in NGC 330 are similar to those in the Galaxy, hence $N_{V/R}^{\rm NGC\ 330}$ should equal $N_{V/R}^{\rm Gal}$;
2. A weak point in this study is that $N_{V/R}^{\rm GAL}$ is based on field Be stars and is therefore based on an age-averaged sample while $N_{V/R}$ of NGC 330 is a representative number for a fixed stellar age of $T = 19$ My (Keller et al. 1999). This becomes important when considering that, at least in the Galaxy, the Be phenomenon occurs in the second half of the main sequence life-time (Fabregat & Torrejón 2000). The relation between w and spectral type of NGC 330 might therefore be different from that of the Galactic sample (Fukuda 1982). This relation depends on the evolution of w during the main sequence life time of $M = 8 - 15\ M_\odot$ stars.
   Recent stellar evolution models for rotating massive stars (Heger et al. 2000; Heger & Langer 2000) indicate that the surface rotation velocity during the main sequence lifetime is reduced by about 10% to 20% of the initial surface rotation velocity:

$$v_2^{\rm equ} = (0.8 \ldots 0.9) v_1^{\rm equ}. \quad (11)$$

   The indices 1 and 2 stand for the zero age main sequence and the termination of the main sequence (more precisely: before the contraction of the core) respectively. Because the stellar radius increases during the main sequence life time by factors of 2–3, the relative equatorial velocity with respect to the critical break-up velocity at the end of the main sequence can be estimated to be

$$w_2 = \frac{v_2^{\rm equ}}{v_2^{\rm crit}} = (0.8 \ldots 0.9)\, w_1 \sqrt{R_2/R_1}, \quad (12)$$

   where $\sqrt{R_2/R_1}$ stands for the evolutionary increase of the stellar radius. Generally, the evolutionary increase of the stellar radius and the slowdown of the equatorial velocity cancel out. This means that evolved Be stars being in the second half of their main sequence life time (as we assume is the case for the Be stars in NGC 330; Fabregat & Torrejón 2000) do not rotate as close to the break-up velocity with respect to the zero age main sequence. We therefore argue that Fukuda's empirical relation for the evolutionary mixed Galactic field Be stars is as a first approximation applicable to NGC 330 and that the occurrence of GDOs in the early-type Be stars is not due to a possible enhanced rotational quadrupole in the stellar potential;
3. The lower metallicity could affect the period of the density waves more strongly than the general formation of GDOs. In this case $N_{V/R}$ might be similar to that for Be stars in the Galaxy, but the periods should

be much longer in the early-type Be stars than in the later type Be stars.

This second test for the hybrid model, the predicted larger period of V/R variability, cannot be performed with the present data set since our observations suffer from the short time coverage of only one year. This means also that our asymmetric line profiles match only one criterion to be classified as a Class 2 profile, namely the asymmetry; the second necessary condition, the long term variability, is not proven yet. The only Galactic Be star known to the authors showing an asymmetric Hα emission line without a cyclical variability is κ CMa (Hanuschik et al. 1996). All other Galactic Be stars with Class 2 profiles are by definition V/R-variable. Given the low spectral resolution we expect V/R variability to be first detected in Be stars with the highest $\Delta V_{\rm p}$ (those with comment d/aa in Table 2): G38, G51, G109, G112, and G114. Four further candidates are G40, G103, G109 and G78 (Hummel et al. 1999).

Our emerging result is that evolutionary enhancement of GDOs as well as a possible weak correlation between metallicity and optically thin line force can be ruled out as an explanation for the occurrence of Class 2 emission lines in early-type Be stars in NGC 330. As the metallicity is reduced, the line force is reduces as well and the confinement radius for GDO increases (O97, his Figs. 1 and 2) for which larger V/R-ratio periods are predicted. So it seems to be quite probable that the reduced momentum mostly impacts the periods of the V/R-variability. In this case Be stars in NGC 330 should be close to the critical curve in the $\eta\epsilon - k_2 f^2$ diagram of O97 with large confinement radii and large V/R-ratio periods.

An observational test would be the continued observation of Be stars in NGC 330 known to exhibit asymmetric emission lines on a once-a-year basis, with a higher spectral resolution. One could derive the mean V/R-ratio periods for the early-type and late-type Be stars in NGC 330 separately and compare the values to the known mean V/R-ratio period for Galactic Be stars of $\bar{P}^{\rm Gal}_{V/R} = 6.8$ years (Copeland & Heard 1963).

7. Conclusions

We observed a sample of 48 Hα emission lines using the VLT Kueyen-FORS2-MXU. We tested a prediction of the hybrid version of the theory of global oscillations in Be star circumstellar disks in the metal-deficient environment of the Be star rich SMC cluster NGC 330. We found that the relative number of Be stars with disks showing global disk oscillations is the same as for Galactic field Be stars. Hence early type Be stars can host a GDO also under conditions of a considerably reduced optically thin line force, in contradiction to predictions of the hybrid model for GDOs. We suppose that the reduced line force in NGC 330 generally does not prevent the formation GDOs but rather increases the confinement radius, which would result in a larger mean cycle time for V/R variations in NGC 330.

Acknowledgements. The funding through "Verbundforschung Astronomie" by the Bundesministerium für Forschung und Technologie BMBF grants 05 AV9WM12, 05 AV9MGA and 05 AV9V0A6 is gratefully acknowledged. We thank the referee John Telting for his valuable comments on the selection effects. We thank the VIRMOS Consortium for cooperation in all matters regarding the Mask Manufacturing Unit.

References

Andrillat, Y. 1983, A&AS, 53, 319
Andrillat, Y., & Fehrenbach, Ch. 1982, A&AS, 48, 93
Banse, K., Grosbol, P. J., & Baade, D. 1991, PASP-CS, 25, 120
Ballereau, D., & Chauville, J. 1989, A&A, 214, 285
Böhnhardt, H. (ed.) 2000, FORS1+2 User Manual, VLT-MAN-ESO-13100-1543/1.5
Conti, G., Chiapetti, L., Mattaini, E., et al. 1999, AstroTechJournal, vol. 2, No. 2
Copeland, J. A., & Heard, J. F. 1963, Publ. David Dunlop Obs. Univ. of Toronto, vol. II, Num. 11, 317
Cox, A. N. (ed.), Allen's astrophysical quantities, fourth Ed., New York (AIP Press, Springer), 2000
Dachs, J., Hanuschik, R., Kaiser, D., & Rohe, D. 1986, A&A, 159, 276
Doazan, V., Sedmak, G., Barylak, M., & Rusconi, L. 1991, ESA-SP-1147
Fabregat, J., & Torrejón, J. M. 2000, A&A, 357, 451
Feast, M. W. 1972, MNRAS, 159, 113
Fukuda, I. 1982, PASP, 94, 271
Garmany, C. D., & Conti, P. S. 1985, ApJ, 195, 157
Grebel, E. K. 1995, Ph.D., University Bonn
Grebel, E., & Richtler, T. 1992, A&A, 253, 359
Grebel, E. K., Richtler, T., & de Boer, K. S. 1992, A&A, 254, L5
Hanuschik, R. W., Kozok, D., & Kaiser, D. 1988, A&A, 189, 147
Hanuschik, R. W., Hummel, W., Dietle, O., & Sutorius, E. 1995, A&A, 300, 163
Hanuschik, R. W., Hummel, W., Sutorius, E., Dietle, O., & Thimm, G. 1996, A&AS, 116, 309
Haser, S. M., Pauldrach, A. W. A., Lennon, D. J., et al. 1998, A&A, 330, 285
Heger, A., Langer, N., & Woosley, E. S. 2000, ApJ, 528, 368
Heger, A., & Langer, N. 2000, ApJ, 544, 1016
Hill, V. 1999, A&A, 345, 430
Hummel, W. 2000a, in IAU Coll., 175, 396
Hummel, W. 2000b, in Proc. SPIE, 4010, 190
Hummel, W., & Hanuschik, R. W. 1997, A&A, 320, 852
Hummel, W., Szeifert, T., Gässler, W., et al. 1999, A&A, 352, L31
Jaschek, C., & Jaschek, M. 1981, The classification of stars (Cambridge University Press)
Keller, S. C., & Bessell, M. S. 1998, A&A, 340, 397
Keller, S. C., Wood, P. R., & Bessell, M. S. 1999, A&AS, 134, 489
Keller, S. C., Bessell, M. S., & DaCosta, G. 2000, AJ, 119, 1748
Kudritzki, R. P., Pauldrach, A., & Puls, P. 1987, A&A, 173, 293

Lindsay, E. M. 1961, AJ, 66, 169
Mazzali, P. A., Lennon, D. J., Pasian, F., et al. 1996, A&A, 316, 173
Mennickent, R. E., Sterken, C., & Vogt, N. 1997, A&A, 326, 1167
Okazaki, A. T. 1991, PASJ, 43, 75
Okazaki, A. T. 1997, A&A, 318, 548 (O97)
Okazaki, A. T. 2000, in IAU Coll., 175, 409
Papaloizou, J. C., Savonije, G. J., & Henriches, H. F. 1992, A&A, 265, L45
Porter, J. M. 1996, MNRAS, 280, L31
Rivinius, Th., Baade, D., Štefl, S., et al. 1988, A&A, 336, 177
Robertson, J. W. 1974, A&AS, 15, 261
Savonije, G. J. 1999, in Cyclic Variability in Stellar Winds, ESO Astrophys. Symp., 337
Savonije, G. J., & Heemskerk, M. H. M. 1993, A&A, 276, 409
Schink, H., Nicklas, H., Harke, R., et al. 2000, Proc. SPIE, 4008, ed. M. Iye, & A. F. Moorwood, 175
Seifert, W., Appenzeller, I., Fürtig, W., et al. 2000, Proc. SPIE 4008, ed. M. Iye, & A. F. Moorwood, 96
Slettebak, A., Collins II, G. W., & Truax, T. 1992, ApJSS, 81, 335
Telting, J. H. 2000, in IAU Coll., 175, 422
Telting, J. H., Heemskerk, M. H. M., Henrichs, H. F., & Savonije, G. J. 1994, A&A, 288, 558
Tucholke, H. J., de Boer, K. S., & Seitter, W. 1996, A&AS, 119, 91
Zorec, J., & Briot, D. 1991, A&A, 245, 150
Zorec, J., & Briot, D. 1997, A&A, 318, 443